Crimson Publishers
Wings to the Research

Review Article

Theoretical Investigation on NHC-Catalyzed [4+1] Cyclization of Aldehyde and Amidoxime to Build 3,5-Disubstituted 1,2,4-Oxadiazole

Nan Lu*

College of Chemistry and Material Science, Shandong Agricultural University, China

ISSN: 2637-8035

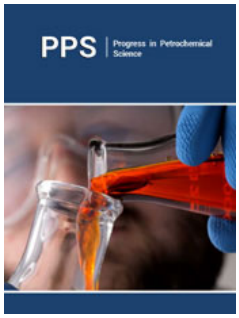

***Corresponding author:** Nan Lu, College of Chemistry and Material Science, Shandong Agricultural University, Taian 271018, PR China

Submission: December 22, 2025
Published: January 12, 2026

Volume 7 - Issue 4

How to cite this article: Nan Lu*. Theoretical Investigation on NHC-Catalyzed [4+1] Cyclization of Aldehyde and Amidoxime to Build 3,5-Disubstituted 1,2,4-Oxadiazole. Progress Petrochem Sci. 7(4). PPS. 000670. 2026.
DOI: 10.31031/PPS.2026.07.000670

Abstract

The first theoretical investigation on NHC-catalyzed [4+1] cyclization of (Z)-N′-hydroxybenzimidamide and p-chlorobenzaldehyde was provided by our DFT calculation. Via deprotonation of triazole salt precursor, the free N-Heterocyclic Carbene (NHC) catalyst was initially generated. Then, via rapid carbene addition to aldehyde followed by proton transfer, the breslow intermediate was afforded and further converted to acyl azolium under oxidation acting as electrophile in the following. Subsequently, with additional amidoxime, the nucleophilic substitution occurs with its nucleophile group leading to ester intermediate. After elimination of recovered HNHC, ester undergoes aza-ring closure and dehydration to construct five-membered aromatic heterocyclic structure of target 3,5-disubstituted 1,2,4-oxadiazole product. The proton transfer affording breslow intermediate of step 3 is determined to be rate-limiting for the whole process.

Keywords: [4 + 1] cyclization; Amidoxime; 1,2,4-oxadiazole; Triazole salt; N-heterocyclic carbene

Introduction

As a class of five-membered heterocyclic compound containing nitrogen, 1,2,4-oxadiazole has been widely used in pharmaceutical industry due to significant structure and unique property. This heterocycle structure in ataluren can treat Duchenne muscular dystrophy, cystic fibrosis nonsense mutation and in tioxazafen as nematicide against parasitic nematode [1,2]. In addition, 1,2,4-oxadiazole skeleton was identified as core structural unit in natural alkaloid such as liquid crystal, energetic and luminescent materials [3-6]. Owing to the significance, the synthesis of 1,2,4-oxadiazole has emerged recently involving reaction between amidoximes and carboxylic acid derivatives and carboxylic acids activated by reagents. Kaboudin reported an efficient method for synthesis of 1,2,4-oxadiazoles in water [7]. Movassagh developed one-pot synthesis of 3,5-disubstituted 1,2,4-oxadiazoles from nitriles mediated by K_3PO_4 [8]. Tolmachev discovered expanding synthesizable space of disubstituted 1,2,4-oxadiazoles [9]. Sharonova gave facile room-temperature assembly of 1,2,4-oxadiazole core from amidoximes and carboxylic acids [10]. However, these approaches require harsh reaction condition of high temperature and complex purification with low yield and limited substrate scope.

N-Heterocyclic Carbenes (NHCs) are well-known effective organic catalysts in constructing oxygen and nitrogen-containing heterocycle. In this field, Zhang researched asymmetric synthesis of γ-lactams under low-loading N-heterocyclic carbene catalysis [11]. Kowalska achieved harnessing indole-derived hydrazones for enantioselective synthesis

of pyrroloindolones via NHC-catalyzed formal [3+2]-cycloaddition [12]. Wu obtained N-heterocyclic carbene-catalyzed [3+3] annulations to access dihydropyrano [3,2-b] pyrrol-5-ones [13]. There was also [3+3] annulation of enals and oxindole-derived enals with 2-aminoacrylates, enantioselective synthesis of dihydrothiopyranones of 2-bromoenals with β-oxodithioesters and preparation of 4,6-disubstituted α-pyrone [14-16]. When it comes to five-membered aromatic heterocycle, the construction of 2-aminofuran-3-carbonitriles via cascade stetter-γ-ketonitrile cyclization, 2-aryl indoles, 1,2,3-triazoles via intermolecular cross-couplings of azides and LUMO-activated unsaturated acyl azoliums and substituted imidazoles from aryl methyl ketones and benzylamines has also been achieved via NHC catalysis [17-20]. This progress offers novel insights to heterocyclic synthesis. Among conventional methods constructing 1,2,4-oxadiazole, Saadati realized manganese oxide nanoparticles supported on graphene oxide as nanocatalyst from aldehydes [21]. Basak gave convenient one-pot synthesis of 2,4,6-triarylpyridines using graphene oxide as metal-free catalyst with dual catalytic activity [22]. Since few reports documented NHC catalysis for heterocycle, Fu group has done many researches such as NHC catalyzed desymmetrization of N-Cbz glutarimides and oxidation of aldehydes to esters [23,24].

The latest breakthrough was NHC-catalyzed [4+1] cyclization of (Z)-N′-hydroxybenzimidamide and p-chlorobenzaldehyde [25]. Although 3,5-disubstituted 1,2,4-oxadiazole was synthesized, how free N-heterocyclic carbene was generated from selected triazole salt precursor? What's the concrete process to form key breslow intermediate involving carbene addition and proton transfer? How acyl azolium acts as electrophile undergoing nucleophilic substitution followed by aza-ring closure and dehydration producing target product?

Computational Details

Structures were optimized at M06-2X/6-31G(d) level with GAUSSIAN09 [26]. Among various DFT methods [27], M06-2X functional has smaller deviation between experimental and calculated value than B3LYP hybrid functional [28,29]. With 6-31G(d) basis set, it can provide best compromise between time consumption and energy accuracy. It was also found to give accurate results for stepwise (2+2) cycloaddition, enantioselective (4+3) and Diels-Alder reaction [30,31]. Together with good performance on noncovalent interaction, it is suitable for this system [32-34]. To obtain Zero-Point Vibrational Energy (ZPVE), harmonic frequency calculations were carried out at M06-2X/6-31G(d) level gaining thermodynamic corrections at 298K and 1atm in acetonitrile (CH_3CN). At M06-2X/6-311++G(d,p) level, the solvation-corrected free energies were obtained using Integral Equation Formalism Polarizable Continuum Model (IEFPCM) [35-39] on M06-2X/6-31G(d)-optimized geometries. NBO procedure was performed with Natural Bond Orbital (NBO3.1) obtaining lone pair and bond to characterize bonding orbital interaction and electronic properties [40-42]. Using Multiwfn_3.7_dev package [43].

Results and Discussion

The mechanism was explored for NHC-catalyzed [4+1] cyclization of (Z)-N′-hydroxybenzimidamide 1 and p-chlorobenzaldehyde 2 leading to 3,5-disubstituted 1,2,4-oxadiazole 3 (Scheme 1). As is illustrated by black arrow of Scheme 2, first, the deprotonation of triazole salt precursor generates free NHC catalyst. Then, the rapid carbene addition to aldehyde 2 together with proton transfer gave key breslow intermediate which further converted to acyl azolium acting as an electrophile in the following. Next, the nucleophilic substitution occurs with nucleophile group in amidoxime 1. Finally, ester intermediate is obtained after the elimination of HNHC, which undergoes aza-ring closure and dehydration within the reaction system to construct five-membered aromatic heterocyclic structure of target product 3. Figure 1 listed schematic structures of optimized TSs in Scheme 2. Table 1 gave activation energy for all steps.

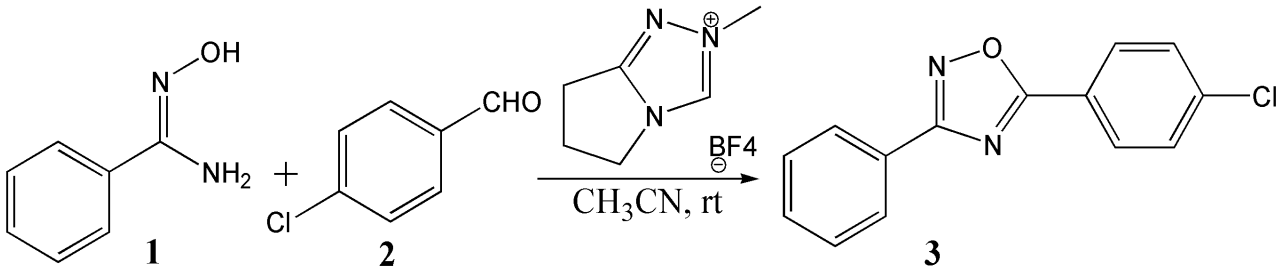

Scheme 1: NHC-catalyzed [4+1] cyclization of (Z)-N′-hydroxybenzimidamide 1 and p-chlorobenzaldehyde 2 leading to 3,5-disubstituted 1,2,4-oxadiazole 3.

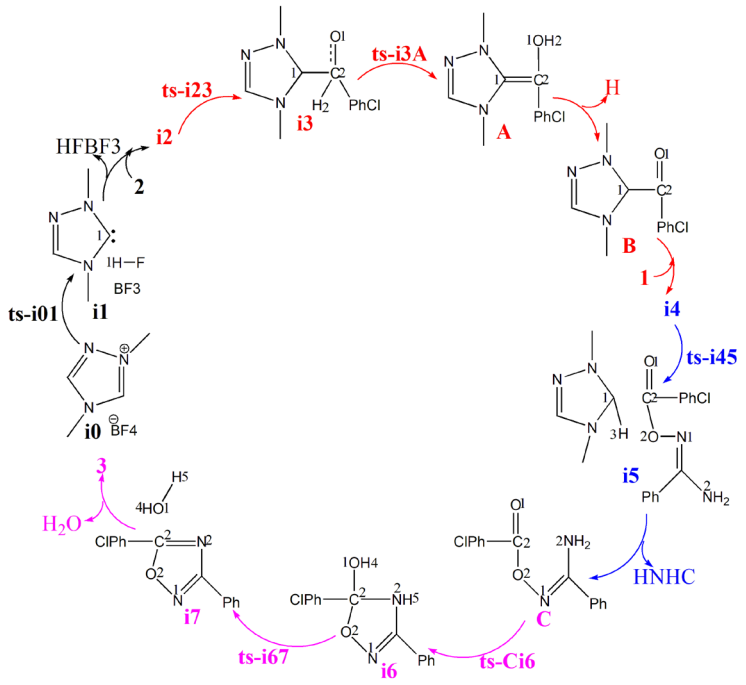

Scheme 2: Proposed reaction mechanism of NHC-catalyzed [4+1] cyclization of 1 and 2 to build 3. TS is named according to the two intermediates it connects.

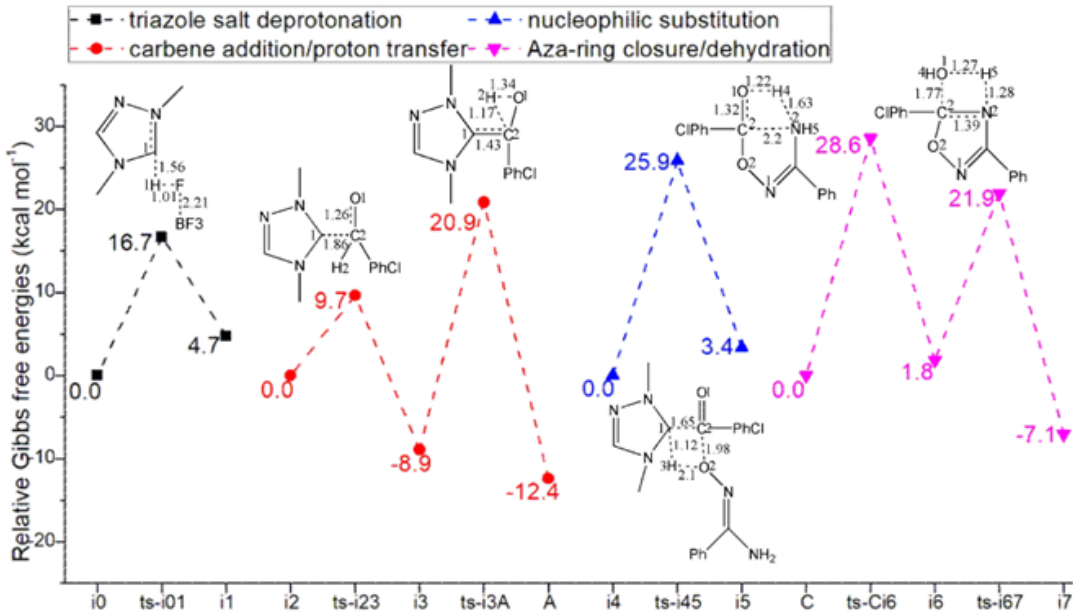

Figure 1: Relative Gibbs free energy profile in solvent phase starting from complex i0, i2, i4, C (bond lengths of optimized TSs in Å).

Table 1: The activation energy (in kcal mol^{-1}) of all reactions in gas and solvent.

TS	$\Delta G^{\neq}_{gas}$	$\Delta G^{\neq}_{sol}$
ts-i01	14.0	16.7
ts-i23	10.7	9.7
ts-i3A	25.5	29.8
ts-i45	26.9	25.9
ts-Ci6	26.8	28.6
ts-i67	23.6	20.1

Triazole salt deprotonation/carbene addition/proton transfer

In step 1, the deprotonation of triazole salt precursor denoted as i0 occurs via ts-i01 with the activation energy of 16.7kcal mol^{-1} endothermic by 4.7kcal mol^{-1} producing free NHC catalyst binding with HF and BF_3 in i1 (black dash line of Figure 1). The transition vector corresponds to proton H1 on methyl group of cations captured by F of BF_4 anion denoted as C1···H1···F along with concerted breaking of B···F (1.56, 1.01, 2021 Å). Once HF molecule

is generated, other two parts formed are also neutral BF_3 and NHC with lone electron pair located on C1 reactive for next step. Then, the intermediate i2 binding NHC and aldehyde 2 is taken as new starting point of next two steps (red dash line of Figure 1). The rapid carbene addition to 2 takes place via ts-i23 with reduced activation energy of 9.7kcal mol^{-1} exothermic by -8.9kcal mol^{-1} in step 2. The transition vector is simple involving C1···C2 bonding and resultant elongation of C2-O1 from double to single (1.86, 1.26 Å) (Figure S1a). The intermediate B is stable with typical C1-C2 single bond. The subsequent proton transfer is required to afford key breslow intermediate A. Via ts-i3A in step 3, the activation energy is increased to be 29.8kcal mol-1 continuously exothermic by -12.4 kcal mol^{-1}. From detailed atomic motion of transition vector, the proton H2 shifts from C2 to O1 that is C2···H2···O1 as well as enhanced C1-C2 from single to double (1.17, 1.34, 1.43 Å) (Figure S1b). With formal hydroxyl O1H2 and C1=C2 double bond, the breslow intermediate A is delivered, which further converted to acyl azolium B under oxidation acting as an electrophile in the following. After removing H2, C2-O1 contracted as double bond with recovered C1-C2 single one in B (Table S1).

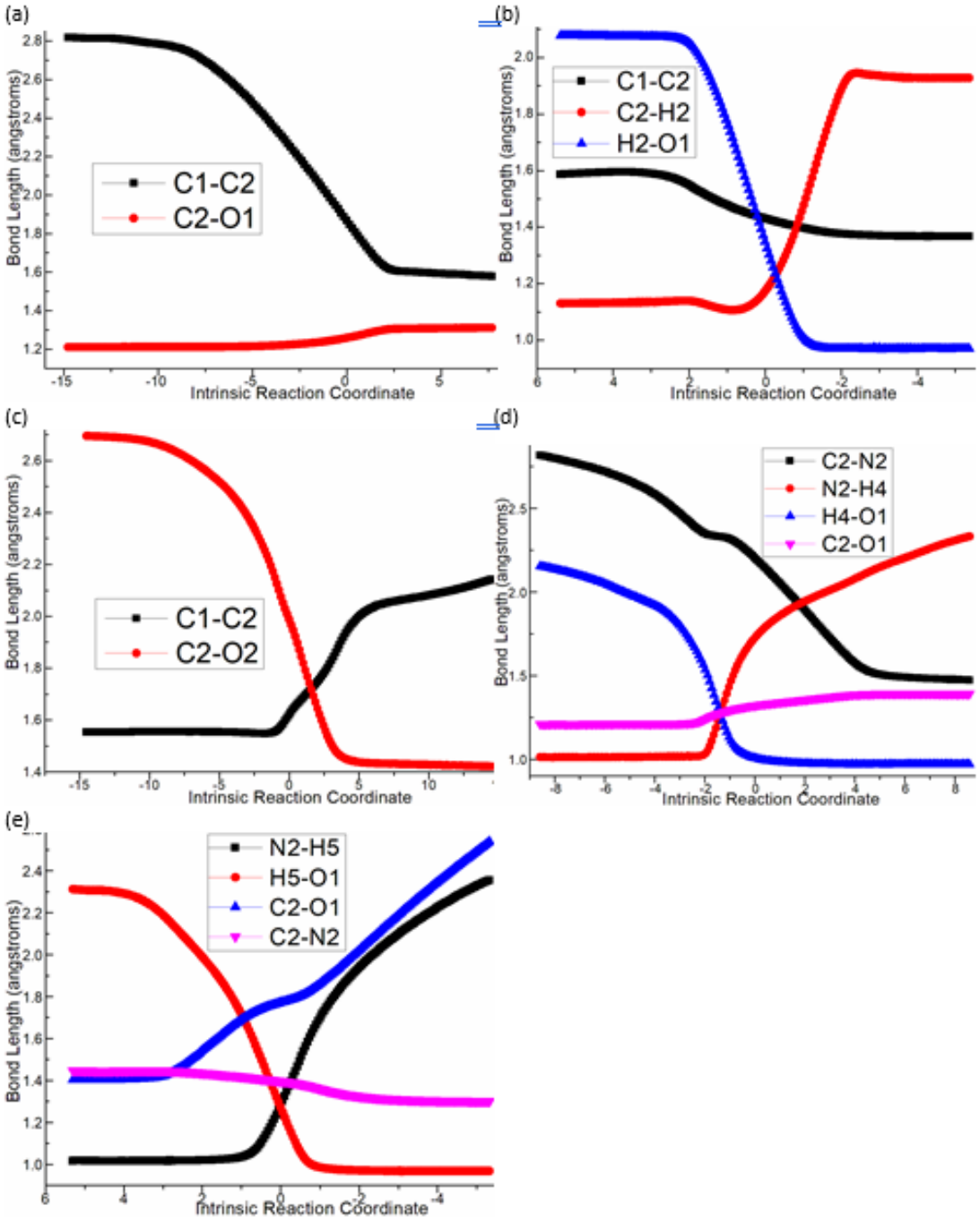

Figure S1: Evolution of bond lengths along the IRC for (a) ts-i23, (b) ts-i3A, (c) ts-i45, (d) ts-Ci6 and (e) ts-i67 at M06-2X/6-311++G(d,p) level.

Table S1: Calculated relative energies (all in kcal mol^{-1}, relative to isolated species) for the ZPE-corrected Gibbs free energies (ΔG_{gas}), Gibbs free energies for all species in solution phase (ΔG_{sol}) at 298 K by M06-2X/6-311++G(d,p)//M06-2X/6-31G(d) method and difference between absolute energy.

Species	ΔG_{gas}	$\Delta G_{sol(CH3CN)}$
i0	0.00	0.00
ts-i01	14.03	16.67
i1	7.53	4.71
nhc+2	0.00	0.00
i2	-2.67	-6.21
ts-i23	8.07	3.45
i3	-9.26	-15.14
ts-i3A	16.26	14.66
A	-12.93	-18.60
nhc+2-h+1	0.00	0.00
i4	0.52	-3.34
ts-i45	27.46	22.52
i5	5.26	0.03
1+2-2h	0.00	0.00
C	-2.95	-6.41
ts-Ci6	23.85	22.17
i6	-1.23	-4.59
ts-i67	22.41	15.51
i7	-9.07	-13.48
1+2-2h-h2o	0.00	0.00
3	1.57	3.04

Nucleophilic substitution/aza-ring closure/dehydration

Next, acyl azolium B and additional amidoxime 1 afford intermediate i4 as new starting point of step 4. With nucleophile hydroxyl O2H3 of 1, the nucleophilic substitution proceeds via ts-i45 with activation energy of 25.9kcal mol^{-1} slightly endothermic by 3.4kcal mol^{-1} giving intermediate i5 (blue dash line of Figure 1). The transition vector suggests facile cleavage of C1···C2 single bond driven by linkage of C2-O2 and transferring of H3 from O2 to C1 (1.65, 1.98, 2.1, 1.12 Å) (Figure S1c). Clearly, the carbene catalyst is readily recovered with C1-H3 as HNHC detaching from the system. After the elimination of HNHC, ester intermediate C is obtained as new starting point of next two steps (magenta dash line of Figure 1). C undergoes aza-ring closure via ts-Ci6 with increased activation energy of 28.6kcal mol^{-1} endothermic by 1.8kcal mol^{-1} in step 5. The transition vector is complicated not only including linkage of C2···N2, proton transfer N2···H4···O1 but stretching of C2-O1 from double to single (2.2, 1.63, 1.22, 1.32 Å) (Figure S1d). The 5-membered ring is yielded with typical C2-N2, C2-O1 single bond and hydroxyl O1H4 in intermediate i6. At last, in step 6, i6 undergoes dehydration within the reaction system via ts-i67 with reduced activation energy of 20.1kcal mol^{-1} exothermic by -7.1kcal mol^{-1} yielding intermediate i7 (Table S2).

Table S2: The activation energy (local barrier) (in kcal mol^{-1}) of all reactions in the gas, solution phase calculated with M06-2X/6-311++G(d,p)//M06-2X/6-31G(d) method.

TS	$\Delta G^{\neq}_{gas}$	$\Delta G^{\neq}_{sol}$
ts-i01 (159i)	14.0	16.7
ts-i23 (188i)	10.7	9.7
ts-i3A (1757i)	25.5	29.8
ts-i45 (1067i)	26.9	25.9
ts-Ci6 (400i)	26.8	28.6
ts-i67 (1746i)	23.6	20.1

The transition vector suggests a second apparent proton H5 transfer from N2 to O1, concerted shortening of C2-N2 from single bond to double and cleavage of C2-O1 (1.28, 1.27, 1.39, 1.77 Å) (Figure S1e). The outcome contains formation of C2=N2 double bond and H_2O molecule leaving from the system. Finally, the target product 3,5-disubstituted 1,2,4-oxadiazole 3 is constructed as a five-membered aromatic heterocyclic structure. Comparatively, the proton transfer affording breslow intermediate in step 3 is determined to be rate-limiting for NHC-catalyzed [4+1] cyclization producing 3,5-disubstituted 1,2,4-oxadiazole.

Conclusion

In summary, the first theoretical investigation was provided by our DFT calculation on NHC-catalyzed [4+1] cyclization reaction between (Z)-N′-hydroxybenzimidamide and p-chlorobenzaldehyde. The free N-Heterocyclic Carbene (NHC) catalyst was initially generated from deprotonation of triazole salt precursor. Then, the key breslow intermediate was afforded via rapid carbene addition to aldehyde followed by proton transfer. The acyl azolium was further given under oxidation acting as electrophile in the following. Next, with additional amidoxime, the nucleophilic substitution occurs with its nucleophile group leading to ester intermediate. After the elimination of recovered HNHC, ester undergoes aza-ring closure and dehydration within the reaction system to build five-membered aromatic heterocyclic structure of target product 3,5-disubstituted 1,2,4-oxadiazole. The proton transfer affording breslow intermediate in step 3 is determined to be rate-limiting for this NHC-catalyzed [4+1] cyclization.

Electronic Supplementary Material

Supplementary data available: [Computation information and cartesian coordinates of stationary points; calculated relative energies for the ZPE-corrected Gibbs free energies (ΔG_{gas}), and Gibbs free energies (ΔG_{sol}) for all species in solution phase at 298K.]

Author Contributions

Conceptualization, Nan Lu; Methodology, Nan Lu; Software, Nan Lu; Validation, Nan Lu; Formal Analysis, Nan Lu; Investigation, Nan Lu; Resources, Nan Lu; Data Curation, Nan Lu; Writing-Original Draft Preparation, Nan Lu; Writing-Review & Editing, Nan Lu; Visualization, Nan Lu; Supervision, Nan Lu; Project Administration, Nan Lu. All authors have read and agreed to the published version of the manuscript.

Funding

This work was supported by Key Laboratory of Agricultural Film Application of Ministry of Agriculture and Rural Affairs, PR China.

Conflict of Interest

The authors declare no conflict of interest

References

1. Pichavant C, Aartsma RA, Clemens PR, Davies KE, Dickson G, et al. (2011) Current status of pharmaceutical and genetic therapeutic approaches to treat DMD. Mol Ther 19(5): 830-840.
2. Walker DP, Graham CR, Miller WH, Koeller KJ (2019) Three step, one-pot process to prepare Thiophene-2-Carbonyl Chloride (TCC), a key raw material in the manufacture of tioxazafen (Nemastrike®). Tetrahedron Lett 60(12): 834-838.
3. Carbone M, Li Y, Irace C, Mollo E, Castelluccio F, et al. (2011) Structure and cytotoxicity of phidianidines A and B: First finding of 1,2,4-oxadiazole system in a marine natural product. Org Lett 13(10): 2516-2519.
4. Francescangeli O, Stanic V, Torgova SI, Strigazzi A, Scaramuzza N, et al. (2009) Ferroelectric response and induced biaxiality in the nematic phase of bent-core mesogens. Adv Funct Mater 19(16): 2592-2600.
5. Fu Z, Su R, Wang Y, Wang YF, Zeng W, et al. (2012) Synthesis and characterization of energetic 3-nitro-1,2,4-oxadiazoles. Chem 18(7): 1886-1889.
6. Li Q, Cui SL, Zhong C, Yuan DX, Dong SC, et al. (2014) Synthesis of new bipolar host materials based on 1,2,4-oxadiazole for blue phosphorescent OLEDs. Dyes Pigments 101: 142-149.
7. Kaboudin B, Malekzadeh L (2011) Organic reactions in water: An efficient method for the synthesis of 1,2,4-oxadiazoles in water. Tetrahedron Lett 52(48): 6424-6426.
8. Movassagh B, Talebsereshki F (2013) Mild and efficient one-pot synthesis of 3,5-disubstituted 1,2,4-oxadiazoles from nitriles mediated by K_3PO_4. Synth Commun 44(2): 188-194.
9. Tolmachev A, Bogolubsky AV, Pipko SE, Grishchenko AV, Ushakov DV, et al. (2016) Expanding synthesizable space of disubstituted 1,2,4-oxadiazoles. ACS Combinatorial Science 18(10): 616-624.
10. Sharonova T, Pankrat'eva V, Savko P, Baykov S, Shetnev A (2018) Facile room-temperature assembly of the 1,2,4-oxadiazole core from readily available amidoximes and carboxylic acids. Tetrahedron Lett 59(29): 2824-2827.
11. Zhang Y, Zhang Y, Guo J, Han J, Zhou X, et al. (2021) Asymmetric synthesis of γ-lactams under low-loading N-heterocyclic carbene catalysis. Org Chem Front 8(18): 5087.
12. Kowalska J, Cieslinski A, Aleman J, Albrecht Ł (2015) Harnessing indole-derived hydrazones for enantioselective synthesis of pyrroloindolones via NHC-catalyzed formal [3+2]-cycloaddition. Adv Synth Catal 367(10): e202500016.
13. Wu YT, Zhang R, Duan XY, Yu HF, Sun BY, et al. (2020) Access to dihydropyrano [3,2-b] pyrrol-5-ones skeletons by N-heterocyclic carbene-catalyzed [3+3] annulations. Chem Commun 56(68): 9854.
14. Zhao LL, Li XS, Cao LL, Zhang R, Shi XQ, et al. (2017) Access to dihydropyridinones and spirooxindoles: Application of N-heterocyclic carbene-catalyzed [3+3] annulation of enals and oxindole-derived enals with 2-aminoacrylates. Chem Commun 53(44): 5985.
15. Barik S, Shee S, Gonnade RG, Biju AT (2022) Enantioselective synthesis of dihydrothiopyranones via NHC-catalyzed [3+3] annulation of 2-bromoenals with β-oxodithioesters. Org Lett 24(48): 8848-8853.
16. Bera S, Studer A (2017) Preparation of 4,6-disubstituted α-pyrones by oxidative N-heterocyclic carbene catalysis. Synthesis 49(1): 121-126.
17. Liu P, Lei M, Ma L, Hu L (2011) An efficient synthesis of 2-aminofuran-3-carbonitriles via cascade stetter-γ-ketonitrile cyclization reaction catalyzed by n-heterocyclic carbene. Synlett 2011(8): 1133-1136.
18. Hovey MT, Check CT, Sipher AF, Scheidt KA (2014) N-heterocyclic-carbene-catalyzed synthesis of 2-aryl indoles. Angew Chem Int Ed 53(36): 9603-9607.
19. Li W, Ajitha MJ, Lang M, Huang K, Wang J (2017) Catalytic intermolecular cross-couplings of azides and LUMO-activated unsaturated acyl azoliums. ACS Catal 7(3): 2139-2144.
20. Alanthadka A, Elango SD, Thangavel P, Subbiah N, Vellaisamy S, et al. (2019) Construction of substituted imidazoles from aryl methyl ketones and benzylamines via N-heterocyclic carbene-catalysis. Catal Commun 125: 26-31.
21. Saadati F, Kaboudin B, Hasanloei R, Namazifar Z, Marset X, et al. (2020) Manganese oxide nanoparticles supported on graphene oxide as an efficient nanocatalyst for the synthesis of 1,2,4-oxadiazoles from aldehydes. Appl Organomet Chem 34(10): e5838.
22. Basak P, Dey S, Ghosh P (2021) Convenient one-pot synthesis of 1,2,4-oxadiazoles and 2,4,6-triarylpyridines using Graphene Oxide (GO) as a metal-free catalyst: Importance of dual catalytic activity. RSC Adv 11(51): 32106-32118.
23. Hu Z, Wei C, Shi Q, Hong X, Liu J, et al. (2022) Desymmetrization of N-Cbz glutarimides through N-heterocyclic carbene organocatalysis. Nat Commun 13(1): 4042.
24. Sarkar DS, Grimme S, Studer A (2010) NHC catalyzed oxidations of aldehydes to esters: Chemoselective acylation of alcohols in presence of amines. J Am Chem Soc 132(4): 1190-1191.
25. Zhu H, Fu Z (2025) NHC-catalyzed synthesis of 3,5-disubstituted 1,2,4-oxadiazoles from amidoximes and aldehydes. Org Lett 27(46): 12835-12839.
26. Frisch MJ, Trucks GW, Schlegel HB, Scuseria GE, Robb MA, et al. (2010) Gaussian 09 (Revision B.01). Gaussian Inc, Wallingford, Connecticut, UK.
27. Stephens PJ, Devlin FJ, Chabalowski CF, Frisch MJ (1994) Ab initio calculation of vibrational absorption and circular dichroism spectra using density functional force fields. J Phys Chem 98(45): 11623-11627.
28. Becke AD (1996) Density-functional thermochemistry. IV. A new dynamical correlation functional and implications for exact-exchange mixing. J Chem Phys 104(3): 1040-1046.
29. Lee CT, Yang WT, Parr RG (1998) Development of the collesalvetti correlation-energy formula into a functional of the electron density. Phys Rev B Condens Matter 37(2): 785-789.

30. Li X, Kong X, Yang S, Meng M, Zhan X, et al. (2019) Bifunctional thiourea-catalyzed asymmetric inverse-electron-demand diels-alder reaction of allyl ketones and vinyl 1,2-diketones via dienolate intermediate. Org Lett 21(7): 1979-1983.

31. Krenske EH, Houk KN, Harmata M (2015) Computational analysis of the stereochemical outcome in the imidazolidinone-catalyzed enantioselective (4+3)-cycloaddition reaction. J Org Chem 80(2): 744-750.

32. Lv H, Han F, Wang N, Lu N, Song Z, et al. (2022) Ionic liquid catalyzed c-c bond formation for the synthesis of polysubstituted olefins. Eur J Org Chem 2022(45): e202201222.

33. Zhuang H, Lu N, Ji N, Han F, Miao C (2021) Bu_4NHSO_4-catalyzed direct N-allylation of pyrazole and its derivatives with allylic alcohols in water: A metal-free, recyclable and sustainable system. Advanced Synthesis & Catalysis 363(24): 5461-5472.

34. Lu N, Liang H, Qian P, Lan X, Miao C (2020) Theoretical investigation on the mechanism and enantioselectivity of organocatalytic asymmetric povarov reactions of anilines and aldehydes. Int J Quantum Chem 120(8): e26574.

35. Tapia O (1992) Solvent effect theories: Quantum and classical formalisms and their applications in chemistry and biochemistry. J Math Chem 10: 139-181.

36. Tomasi J, Persico M (1994) Molecular interactions in solution: An overview of methods based on continuous distributions of the solvent. Chem Rev 94(7): 2027-2094.

37. Simkin BY, Sheikhet I (1995) Quantum chemical and statistical theory of solutions: A computational approach. Ellis Horwood, London, New York, USA.

38. Tomasi J, Mennucci B, Cammi R (2005) Quantum mechanical continuum solvation models. Chem Rev 105(8): 2999-3093.

39. Marenich AV, Cramer CJ, Truhlar DG (2009) Universal solvation model based on solute electron density and on a continuum model of the solvent defined by the bulk dielectric constant and atomic surface tensions. J Phys Chem B 113(18): 6378-6396.

40. Reed AE, Weinstock RB, Weinhold F (1985) Natural population analysis. J Chem Phys 83(2): 735-746.

41. Reed AE, Curtiss LA, Weinhold F (1988) Intermolecular interactions from a natural bond orbital, donor-acceptor view point. Chem Rev 88(6): 899-926.

42. Foresman JB, Frisch A (1996) Exploring chemistry with electronic structure methods. (2^{nd} edn), Gaussian Inc, Pittsburgh, USA.

43. Lu T, Chen F (2012) Multiwfn: A multifunctional wavefunction analyzer. J Comput Chem 33(5): 580-592.

